



## SWASH HYDRO-MORPHODYNAMICS AT A LOW-TIDE TERRACE BEACH DURING POST-TYPHOON RECOVERY PERIOD, NHA TRANG BAY, VIETNAM

RAFAEL ALMAR<sup>(1)</sup>, JEAN-PIERRE LEFEBVRE<sup>(1)(2)</sup>, NATALIE BONNETON<sup>(3)</sup>, PHILIPPE BONNETON<sup>(3)</sup>, DINH VAN UU<sup>(2)</sup>, NGUYEN TRUNG VIET<sup>(4)</sup>, LE THANH BINH<sup>(5)</sup>, NGUYEN VIET DUC<sup>(6)</sup>

<sup>(1)</sup> IRD-LEGOS (CNRS/IRD/CNES/Toulouse University), Toulouse, France  
rafael.almar@ird.fr

jean-pierre.lefebvre@ird.fr

<sup>(2)</sup> Hanoi University of Sciences, Hanoi, Vietnam  
uudv50@gmail.com

<sup>(3)</sup> EPOC (CNRS/Bordeaux University), Bordeaux, France  
n.bonneton@epoc.u-bordeaux1.fr

p.bonneton@epoc.u-bordeaux1.fr

<sup>(4)</sup> Water Resources University, Hanoi, Vietnam  
nguyentrungviet@wru.vn

<sup>(5)</sup> Hydraulic Engineering Consultants, Hanoi, Vietnam  
lebinh.hec@gmail.com

<sup>(6)</sup> Central Vietnam Construction and Consultancy, Ha Tinh, Vietnam  
nguyenvietduch1978@gmail.com

### ABSTRACT

Several major typhoons hit the Vietnamese coast every year, inducing punctual dramatic erosions. The post-typhoon wave conditions, dominated by swash processes are thus crucial to reconstruct the beaches. However, only little is known on the swash processes and their contribution to wave energy dissipation and beach evolution. Two field experiments were conducted at Nha Trang; the first in May 2013 during summer monsoon (low energetic oblique wind waves) and the second in December 2013 during winter monsoon (moderate energetic shore-normal swell waves). Specific innovative instrumentation was deployed, based on a combination of cross-shore video poles, micro-ADV profiler and pressures sensors to study the swash hydrodynamic processes and associated bed evolution. This setup allowed describing the wave energy transfers, dissipation and reflection in the swash, swash-induced current, as well as to understand the individual wave/group impact on bed evolution. This study contribute in addressing the questions of integrated contribution of small-scale swash processes to the overall shoreface evolution (equilibrium concept) as well as energy balance (low frequency swash filter).

*Keywords:* wave reflection and dissipation; low energy environments, swash video poles, wind-waves, typhoon impact

### 1. INTRODUCTION

Beaches located in semi-enclosed bays, mostly sheltered from the action of waves or exposed to strong seasonal modulation, with long periods of moderate wave energy, can be defined as low energy environments (Jackson et al., 2010). In these environments, major morphological changes are believed to be attributed to punctual moderate to high energy wave events, the beach staying mainly inactive between these events. Exchanges between subtidal and upper beach are assumed weak or rather non-existent, as the widely employed depth-of-closure is very small. These environments remained mainly out of the scope of major research interest and their dynamics is not well understood. Particularly, how the beach is able to recover if the subtidal and upper beach sediment cells are disconnected? are the morphological features generated during energetic events really fixed or the weak energetic wave conditions make them to evolve? Beaches impacted by punctual event recover mostly during weak energy

periods which are crucial to describe the behavior of the whole beach dynamics.

The low energy dynamic involved in the beach recovery is dominated by swash dynamics. This dynamic is complex with high levels of turbulence and suspended sediment. Consequently, both cross- and long-shore sediment fluxes are large. For instance, swash processes during low energy wind-waves conditions may be responsible of up to 50% of alongshore drift (Elfrink and Baldock, 2002). Cross-shore transport within the swash zone is complex with large sediment fluxes and small net balance, the difference between accretive and erosive events being determined by complex thresholds. Finally, equilibrium between swash hydrodynamics and shoreface is still under investigation.

Both hydro and morphological swash motions are constantly evolving with wave and tide forcing. Though its key importance, the misunderstanding of swash dynamics is mostly hampered by the difficulties of observation in the field. Recent advances in measurements

techniques made possible the fine measurement at high frequency of water elevation and bed level from LIDAR (see Blenkinsopp et al., 2012; Vouduoukas et al., 2014). Because this technique is costly and post-processing complex, we aimed here at developing a new low cost technique which allows a direct measurement of the swash zone.

In this paper we use the data from two field experiments conducted at a low energy beach, to understand the recovery swash processes. In the second section, the field site is presented; in the third section, the new method of swash measurement recently developed is described; in a third section, the method is validated and results on its application to swash dynamics are presented. Finally discussion and conclusions are given.

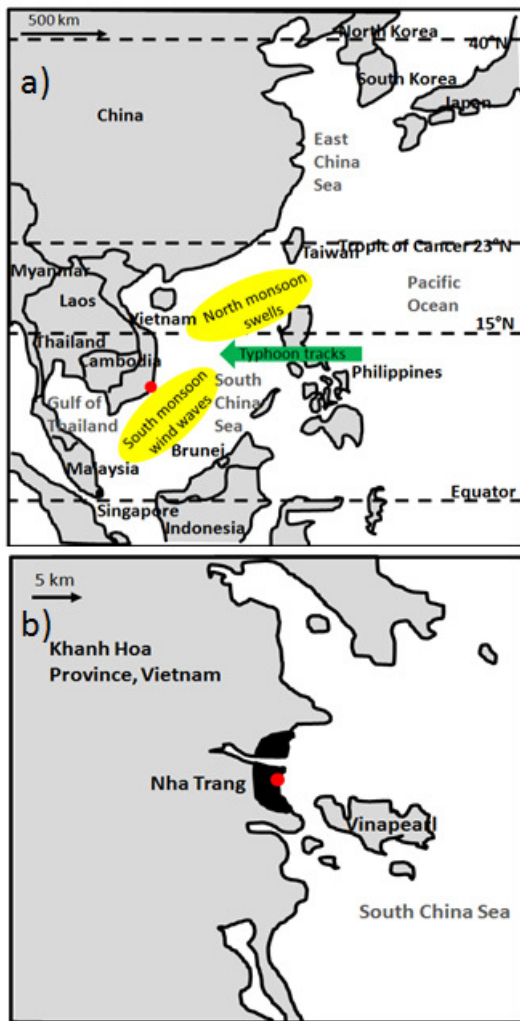


Figure 1. Study area of Nha Trang, Vietnam, South East Asia, at a) regional scale and b) local bay scale.

## 2. STUDY AREA

The study site is Nha Trang Beach (12°N, 109°E), South East of Vietnam in the Khanh Hoa Province, facing the fetch limited South China Sea (Figure 1.a). This beach has been identified by the Vietnamese government as a priority for the development of tourism. Wave climate is characterized by a large seasonal variation; the wave regime being dominated by wind wave, oriented South, during the south summer monsoon, from March to September, and dominated by North-East swell waves during the North winter monsoon from October to

February. This region is the most cyclogenesis in the world and 4 to 6 typhoons hit the coast every year (Nicholls et al. 1999) from October to December. This rugged coastline is characterized by sandy/mud mixed environment.

The 7-km long Nha Trang embayed beach is oriented North-South (Figure 1.b), sheltered from South-East to South incident waves by the Vinepearl Island and disrupted at its center part by the Cai river mouth. Sediment on the shoreface is medium sized ( $D_{50}=300 \mu\text{m}$ ). The beach is a mixed wave-dominated micro-tidal environment (Relative Tidal Range  $RTR \sim 1$ ), tide being mixed to diurnal. Beach morphology presents a strong variability but remains mostly in an alongshore uniform intermediate low-tide terrace reflective upper beach state (Gourlay parameter  $\Omega \sim 1.5$ ).

Two field experiments were conducted at Nha Trang Beach in 2013 (Figure 2); the first one from 26th to 30th May and the second one from 3rd to 10th December. First campaign (NT1) aimed at describing south summer monsoon wind-wave dominated dynamics, while the second experiment (NT2) aimed at better understanding the more energetic swell-wave dominated dynamics. Deployments during the two experiments were similar, with 2 AWACs in 10 m and 5-6 m deep water, current-meter in 3-m water depth for wave and tide forcing, and refined surf-zone and swash measurements; swash video-poles (see next Section for a description) and Nortek Vectrino II micro-profiler. During NT2, 4 synchronized 8Hz-pressure sensors were deployed additionally for swash pole technique validation. A bathymetric survey was undertaken at the beginning of the experiment while the upper beach changes were monitored from daily theodolite surveys.

To complement these intensive short-term experiments, a two-camera permanent video system was deployed in March 2013 (see Viet et al., 2014a,b; Lefebvre et al., 2014). 15-min secondary images (timestacks, time-averaged) allow extracting numerous hydro (waves, current, tide) and morphological parameters (upper beach morphology, bathymetric inversion, shoreline, beach volume).

During the NT1 experiment, tidal range varied from 0.8 to 1.5 m, while the diurnal modulated (i.e. afternoon sea breeze) wind-waves remained roughly constant over the experiment with  $H_s=0.25 \text{ m}$ ,  $T_p=3.3 \text{ s}$  from South-East direction. Beach profiles (Figure 3.a) showed no substantial change, with a spring high-tide mark beach step and a rather linear swash zone, presenting a reflective large 0.17 slope.

During the NT2 experiment, tidal range varied from 1.7 m at spring tide to 0.6 m at neap tide. Swell-wave showed quasi constant characteristics with  $H_s \sim 1 \text{ m}$  and  $T_p \sim 8 \text{ s}$  from shore-normal East direction. Noteworthy, the mega typhoon Haiyan hit the coast on November 14, about 2 weeks before the beginning of the experiment and even if wave energy during NT2 was still moderate for this site, beach was recovering. Alongshore-averaged beach profile (Figure 3.b) showed an almost constant 0.15 slope throughout the experiment, while morphology changed from linear to convex shape.

### 3. VIDEO SWASH POLES MEASUREMENTS

#### 3.1 Data collection

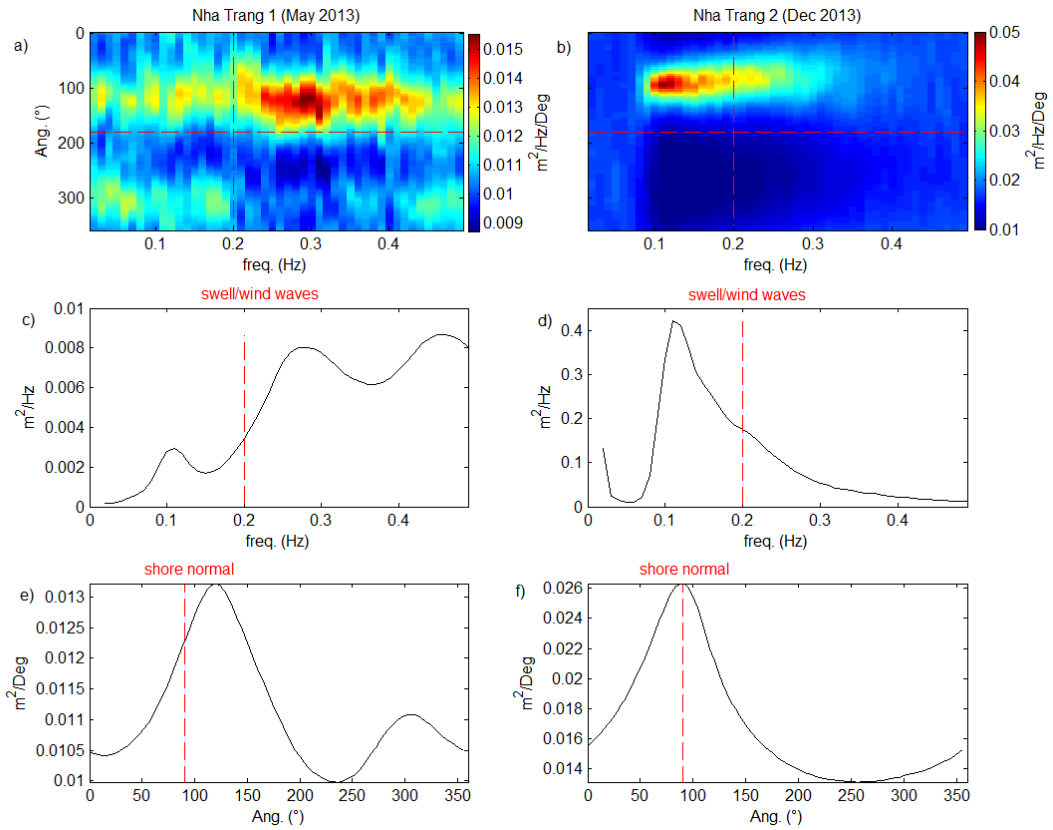


Figure 2. Wave characteristics during NT1 (left column) and NT2 (right column) from 10-m depth AWAC measurements. Upper panels are directional wave spectra, mid panels are distribution in frequency, and bottom panels distribution in angle.

20 metal black painted poles (2-m high, 0.03 m of diameter) are deployed along a cross-shore transect (Figure 4), every 1 m, covering both surf and swash zone. A video camera, (SONY CX-240) full HD (1920x1080 pixels) and high frequency (25 Hz) deployed at the high tide mark, monitors the pole line. Vertical array of pixels on each pole are stacked over time. This was done during daylight hours over the experiments' duration.

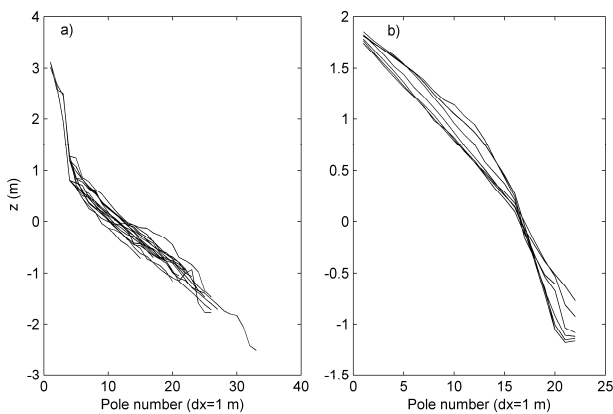


Figure 3. Daily theodolite topographic profiles during a) NT1 and b) NT2.

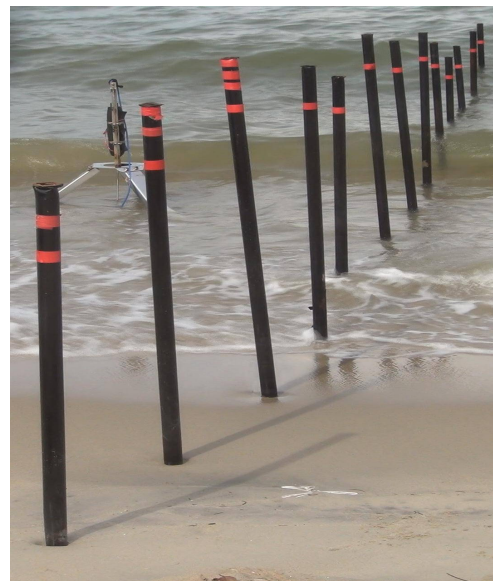


Figure 4. Swash camera view field where poles are visible as well as micro-ADV profiler (NT1).

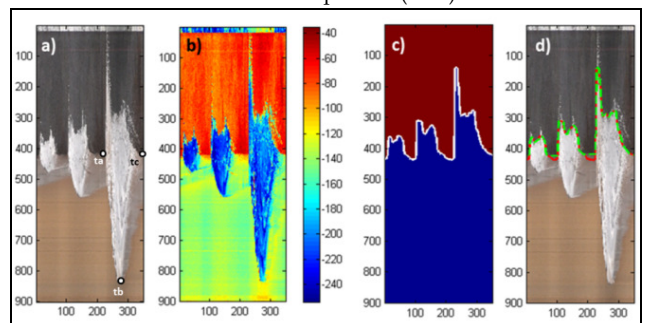


Figure 5. a) 3 swash event original Timestack b) Pixel intensity c) Binary values and its contour d) Timestack with (red) detected contour and (green dashed) corrected contour. From Ibaceta et al., 2014a.

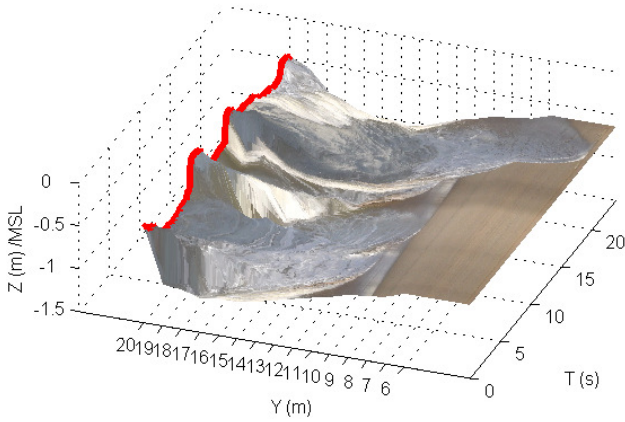


Figure 6. Illustration of a 20 s tridimensional results from video swash poles measurements. Red line stands for elevation at the outer pole (surf).

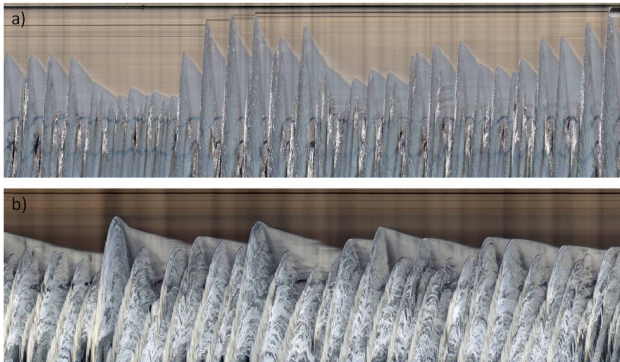


Figure 7. 3-min cross-shore horizontal swash timestacks during a) NT1 and b) NT2.

### 3.2 Image processing

Timestack images are processed to extract water surface and bed elevation. RGB (Red Green Blue) images are converted in intensity values (Figure 5.b) and thresholds are applied to detect the interface (Figure 5.c). Bed and water surface are later distinguished from their temporal characteristics; interface values that don't move within a given duration, typically 1 s, are considered as bed, the rest being moving water (Figure 5.d).

### 3.3 Rectification

The extracted timeseries are visually cross-checked on timestack images to control the quality of the detection. Finally, rectification into real world coordinate is done. Resolution (m/pixel) is given by the number of pixels covered by each pole of known 3-cm diameter. Resolution decreases with the distance to the camera and ranges typically from 0.001 to 0.003 m/pixel. Referencing to the real world coordinates is done relatively to the top of the poles which locations were measured using a theodolite. Final dataset have spatial resolution of 1 m, 0.01 m in the

horizontal and vertical directions, with a temporal resolution of 25 Hz (see Figure 6). Noteworthy, because the data are based on optical video, it is possible to distinguish turbulent from non-turbulent water pixels, and dry from saturated wet sand for bed pixels.

Cross-shore timestacks aligned with poles' transect were also generated (Figure 7) to add a fine description of cross-shore wave dynamics such as bore propagation celerity and runup.

## 4. RESULTS

### 4.1 Video swash pole validation

Co-localized pressure sensors deployed during NT2 were used to validate the video swash pole technique, both in the surf and the swash. A 30 minutes period was chosen for which both video and pressure data were available, on 5 December 2013, from 15h to 15h30. Comparison in Figure 8 shows good agreement. The RMS average error is 0.02 m in the surf (Figure 8.a) and 0.03 m in the swash (Figure 8.c), respectively. As underlined by Cox and Shin (2003), most of the discrepancy rises from difference between direct surface elevation of the video and hydrostatic-based estimation of the pressure sensor; largest differences are observed at the wave front, while back face of the waves show better agreement. Error in the wave front is mainly due to the presence of void in the water column, making the pressure sensor to underestimate roller height. Some errors may also come from the intrusive effects of the video swash poles with the incoming bore splash and backwash. Noteworthy, a sensitivity analysis (not shown here) indicates that the backwash effect has only a weak signature and do not affect surface detection.

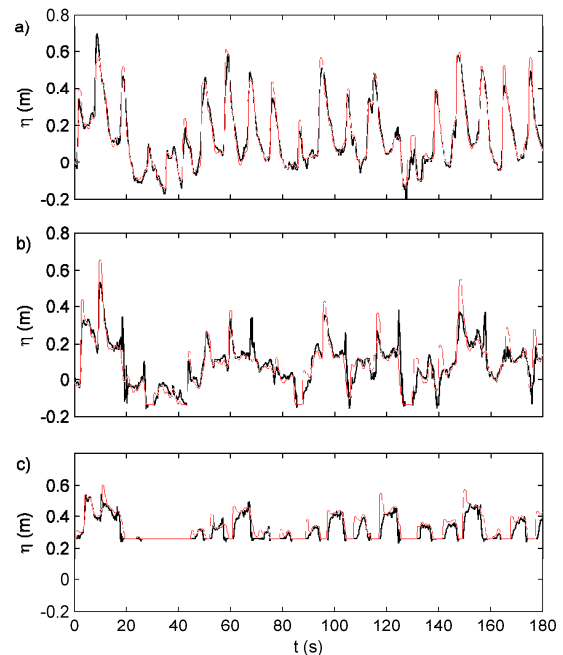


Figure 8. NT2. Comparison between co-localized pressure sensors (black) and swash video pole (red) surface elevation from surf zone to mid-swash (from top to bottom)

## 4.2 Wave transformation and energy dissipation in the swash zone

The swash pole data were analyzed over two 30-min periods, on May 29 15h and December 5 15h for NT1 & NT2, respectively. For each wave passing at the poles, the time and elevation of three points, a, b and c are stored: the initial front time and prior-to-event bed elevation ( $t_a, z_a$ ; see Figure 5.d), time and height of maximum swash ( $t_b, z_b$ ), and end-of-swash time and bed elevation ( $t_c, z_c$ ). An ensemble averaging was conducted (Figure 9.a) over all the waves identified during these 30-min. The wave ensemble-averaged profiles in Figure 9 clearly show the non-linear wave transformation and the difference of dynamics between wind waves of NT1 and swell waves of NT2. NT2 case shows a quasi-systematic occurrence of merging and an asymmetrization (steeper front) of the swash shape while propagating in the SZ, whereas no such behavior appears for NT1.

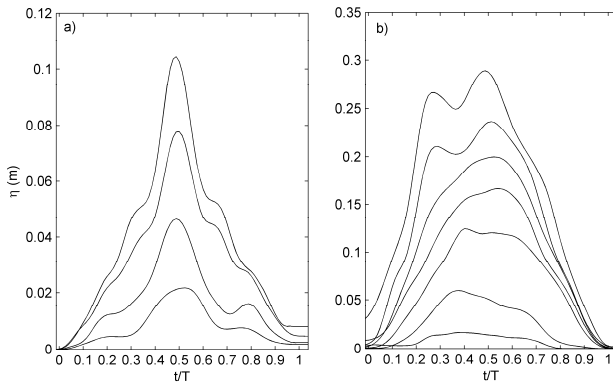


Figure 9. Swash ensemble averaged surface elevation (in m) over a normalized swash period from video poles located in the swash for a) NT1 and b) NT2. Wave transformation can be seen.

Figure 10 shows the energy spectra at the onset of SZ and mid-SZ for NT1 and NT2. In Figure 10.a can be seen the two wind- and swell-wave components at the onset of breaking. The wind-wave energy mostly dissipates in the swash. In Figure 10.b corresponding to the NT2 case, swell-waves are predominant but large infragravity energy is clearly visible at the onset of SZ. This infragravity energy becomes dominant in the SZ due to larger swell-wave dissipation (breaking, turbulence) and transfer from gravity to the infragravity band (Van Dongeren et al., 2007; De Bakker et al., 2013). These results for NT1 and NT2 are also visible in the stack images (Figure 7).

This energy dissipation in the SZ can be linked with outgoing deep water wave energy spectra in Figure 2. The swash zone acts as a low-pass filter for reflected signal where the cut-off frequency depends on local Irribarren number: swash-zone slope and incoming wavelength (Almar et al., 2012; Almar et al., 2014). Here, it can be hypothesized that swell-waves reflection is higher for the NT1 case where SZ slope is in equilibrium with wind-wave (non-saturated swash: swell-waves are in non-saturated conditions, following the Miche (1951) parameter; see Baldock and Holmes, 1999) whereas the shoreface is in equilibrium with swell-wave induced swash in the NT2 case and dissipates most of the

incoming energy in that frequency band. For the NT2 case, only infragravity waves are reflecting (see Figure 10.b). However, these dissipation and reflection aspects have to be further investigated in further details to be confirmed.

## 4.3 Wave-by-wave impact on shoreface

For NT1 and NT2 datasets, the poles located at approximated the 50% swash exceedences were used to illustrate the evolution of the bed level at the individual wave scale. This was done over 10-min periods (Figure 11). Individual wave impact was quantified as  $dz = z_c - z_a$ . Over the studied periods, overall observed bed level changes were +0.01 and +0.02 m for the NT1 and NT2 cases, respectively. As reported in the literature, the complexity of the swash dynamics makes the characterization of the link between bed changes with individual swash characteristics a challenging task (Brochini and Baldock, 2008; Blenkinsopp et al., 2010). Finally, these studies reported that the impact of individual waves seems partly random (Turner et al., 2009). In line with these previous studies, our data from NT1 and NT2 and show large individual wave changes (Figures 11.b, d), in the order of centimeters though the time-integrated evolution is weak. A study is currently conducted on the characterization of this link, to understand the contribution of individual waves to the evolution of the beach profile (Ibaceta et al., 2014a,b).

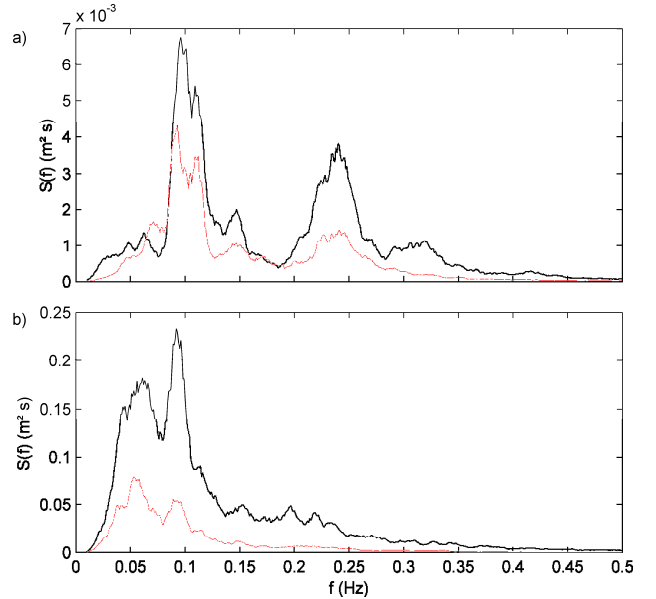


Figure 10. Wave energy spectra derived from video swash poles at swash inception (black) and mid-swash (red) for a) NT1 and b) NT2.

## 4.4 Swash-driven current

During NT1 and NT2, (see Figure 2), the wave incidence was oblique and mostly shore-normal, respectively. The same swash events used in the ensemble averaging defined in previous section are used here to describe the current over a normalized period. First preliminary analyses show that the oblique wave-incidence observed during NT1 generates a current component oriented toward the North (Figure 12.a) whereas no such alongshore component is observed for NT2 (Figure 12.b). This swash-driven alongshore current and consequent

sediment transport might play a key role in Nha Trang beach recovery during the low-energy summer monsoon.

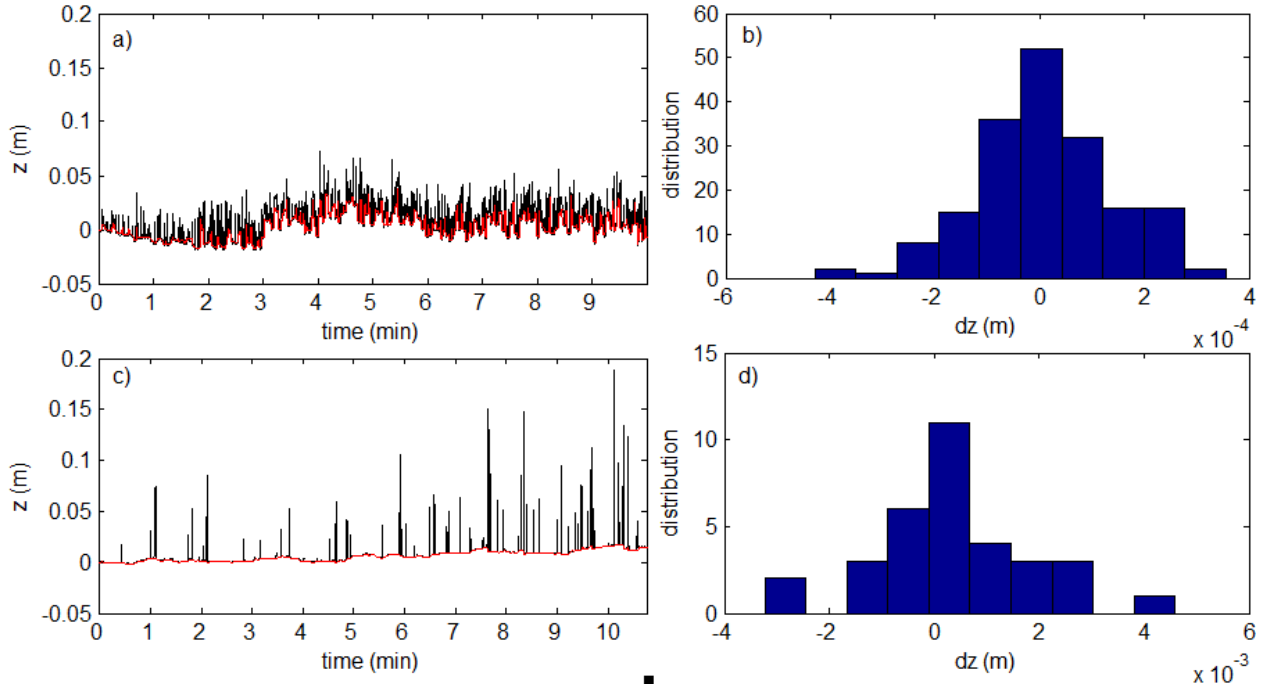


Figure 11. Swash-by-swash bed elevation. left column shows 10-min timeseries of bed (red) and water level (black), right column distribution of individual  $dz$  for (up) NT1 and (down) NT2.

## 5. CONCLUSIONS

Swash measurements from two experiments conducted in 2013 at Nha Trang beach, Vietnam are presented. Swash is thought to play a key role in the recovery of that beach, eroded by typhoons and winter monsoon energetic wave conditions. A new method is introduced that allows a high frequency and high resolution measurement of individual swash and bed evolution. This method is based on the video observation of poles deployed along cross-shore transects in the swash zone.

Our observations in deep water during the two experiments show a contrasted wave forcing; the first experiment (NT1) experiment being characterized by oblique wind-waves whereas the second experiment by shore-normal swell-waves (NT2). While compared to pressure sensors, the video swash pole techniques shows good accuracy in retrieving surface elevation both in the surf and swash zones. Swash measurements show the large difference of dynamics during the two experiments; wind-waves are dissipated whereas swell-waves partly reflect in NT1, and swell-waves dissipate and infragravity reflect in NT2. This argues in favor of a swash zone equilibrium concept; the swash playing the role of low frequency filter with a cut-off frequency that depends on instant beach slope and incident wavelength. Individual bed evolution shows, in line with previous studies, that wave-by-wave impact is hardly predictable, which make its link with macro beach evolution challenging. Finally, this swash-driven dynamic might be responsible for the slow beach post-typhoon recovery. Current research is still going on to address this equilibrium concept and the link between individual wave impact and beach evolution.

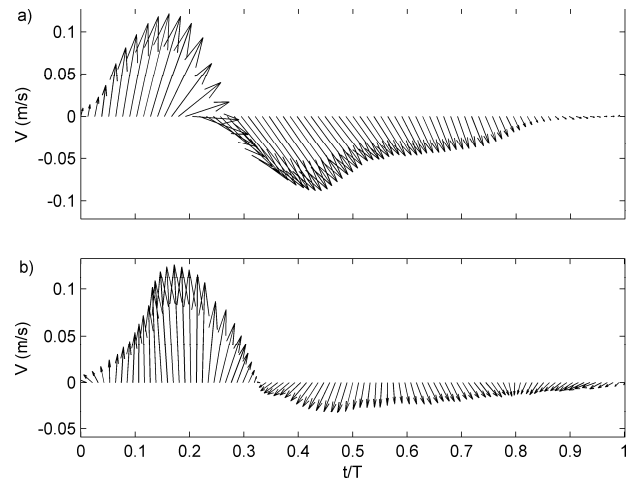


Figure 12. Swash ensemble-averaged current  $V$  (intensity in m/s and direction; the vertical being the cross-shore direction positive toward the beach) from micro-ADV profiler over a normalized swash period for a) NT1 and b) NT2.

## ACKNOWLEDGMENTS

The work described in this publication was supported by the Vietnamese Ministry for Science and Technology (BKHCN/NDT-HD/2013/110). We thank the National Institute of Oceanography of Nha Trang for its help in the preparation and carrying out of this field experiment. The authors also thank the Université des Sciences et des Technologies de Hanoi (USTH) for the use of the VECTRINO II currentmeter. RA funded by INSU/CNRS EC2CO and LEFE projects.

## REFERENCES

- Almar, R., Du Penhoat, Y., Honkonnou, N., Castelle, B., Laibi, R., Anthony, E., Senechal N., Degbe, G., Chuchla, R., Sohoul, Z., Dorel, M., 2014. *The Grand Popo experiment, Benin*, Journal of Coastal Research, SI 70, 651-656, ISSN 0749-0208
- Almar, R., Cienfuegos, R., Gonzalez, E., Catalan, P.A., Michallet, H., Bonneton, P., Castelle, B., Suarez, L., 2012. *Barred-beach morphological control on infragravity motion*, International Conference on Coastal Engineering, Santander, Spain, 2-6 July 2012
- Baldock, T. and Holmes, P., 1999. *Simulation and prediction of swash oscillations on a steep beach*. Coastal engineering, 36, 219-242.
- Blenkinsopp, C.E., Turner, I.L., Allis, M.J., Peirson, W.L. and Garden, L.E., 2012. *Application of LiDAR technology for measurement of time-varying free-surface profiles in a laboratory wave flume*. Coastal Engineering, 68, 1-5.
- Brocchini, M., & Baldock, T. E., 2008. *Recent advances in modeling swash zone dynamics: influence of surf-swash interaction on nearshore hydrodynamics and morphodynamics*. Reviews of Geophysics, 46 (RG3003)
- Cox, D.T., Shin, S., 2003. *Laboratory Measurements of Void Fraction and Turbulence in the Bore Region of Surf Zone Waves*. Journal of Engineering Mechanics, Vol. 129, No. 10
- De Bakker, A., Tissier, M., Marieu, V., Sénéchal, N., Ruju, A., Lara, J. and Ruessink, G., 2013. *Infragravity-wave dissipation on a low-sloping beach*. Proceedings Coastal Dynamics 2013.
- Elfrink, B., Baldock, T., 2002. *Hydrodynamics and sediment transport in the swash zone: a review and perspectives*, Coastal Engineering, 45(3-4), 149-167, ISSN 0378-3839
- Ibaceta, R., Almar, R., Lefebvre, JP. Mensah-Senoo, T., Laryea, W.S., Castelle, B., Senechal, N., du Penhoat, Y. Laibi, R., Hounkonnou, N., 2014. *A new high frequency remote sensing based method: application to the swash zone of a very high reflective beach under high energetic conditions (Grand Popo, Benin)*, Actes des XIIIèmes Journées Nationales Génie Côtier - Génie Civil, Dunkerque 2014, Paralia Editions
- Ibaceta, R., Almar, R., Lefebvre, JP. Mensah-Senoo, T., Laryea, W.S., Castelle, B., Senechal, N., du Penhoat, Y. Laibi, R., Hounkonnou, N., 2014. *High frequency monitoring of swash hydro-morphodynamics on a high-energy low-tide-terraced beach (Grand Popo Beach, Benin, West Africa)*, International Conference on Coastal Engineering, Seoul (Korea), 2014
- Jackson, N.L., Nordstrom, K.L., Eliot, I., Masselink, G. 2002. *'Low energy' sandy beaches in marine and estuarine environments: a review*, Geomorphology, 48(1-3), 147-162
- Lefebvre, J-P, Almar, R., Viet, N.T., Uu, D.V., Thuan, D.H., Binh, L.T, Ibaceta, R., Duc, N.V., 2014. *Contribution of swash processes generated by low energy wind waves in the recovery of a beach impacted by extreme events: Nha Trang, Vietnam*. Journal of Coastal Research, SI 70, 663-668, ISSN 0749-0208
- Miche, R. 1951. *Le pouvoir réfléchissant des ouvrages maritimes exposés à l'action de la houle*. Ann. Ponts Chausses, 121, 285-319
- Nicholls, R.J., Hoozemans, F.M.J., Marchand, M., 1999. *Increasing flood risk and wetland losses due to global sea-level rise: regional and global analyses*, Global Environmental Change, 9, 69-87
- Turner, I.L., Russell, P.E., Butt, T., Masselink, G. & Blenkinsopp, C.E., 2009. *In-situ estimates of net sediment flux per wash: Reply to Discussion by T.E. Baldock of "Measurement of wave-by-wave bed-levels in the swash zone."* Coastal Engineering, doi:10.1016/j.coastaleng.2009.06.001
- Van Dongeren, A.R., Battjes, J., Janssen, T.T., Van Noorloos, J., Steenhauer, K., Steenbergen, G. and Reniers, A., 2007. *Shoaling and shoreline dissipation of low-frequency waves*. Journal of Geophysical Research, 112: doi:10.1029/2006JC003701
- Viet, N.T., Nguyen V.D., Vo C.H., Tanaka H., Dinh V.U, Tran T.T., Almar R., Lefebvre J-P. 2014. *Investigation of Erosion Mechanics of Nha Trang Coast, Vietnam*, IAHR-APD 2014, Hanoi, Vietnam
- Viet,N.T., Nguyen V.D., Le T.B., Duong H.T., Tran T.T., Nguyen V.T, Dinh V.U, Almar R., Lefebvre J-P. and Tanaka, H., 2014. *Seasonal Evolution of Shoreline Changes in Nha Trang Beach, Vietnam*, IAHR-APD 2014, Hanoi, Vietnam
- Vousdoukas, M.I., Kirupakaramoorthy, T., Oumeraci, H., de la Torre, M., Wübbold, F., Wagner, B., Schimmels, S., 2014. *The role of combined laser scanning and video techniques in monitoring wave-by-wave swash zone processes*. Coastal Engineering, Volume 83, January 2014, Pages 150-165, ISSN 0378-3839